Winding angle distributions for random walks and flux lines

Barbara Drossel and Mehran Kardar
Department of Physics, Massachusetts Institute of Technology, Cambridge, Massachusetts 02139
(Received 10 January 1996)

We study analytically and numerically the winding of a flux line around a columnar defect. Reflecting and absorbing boundary conditions apply to marginal or repulsive defects, respectively. In both cases, the winding angle distribution decays exponentially for large angles, with a decay constant depending only on the boundary condition, but not on microscopic features. *Nonuniversal* distributions are encountered for *chiral* defects that preferentially twist the flux line in one direction. The resulting asymmetric distributions have decay constants that depend on the degree of chirality. In particular, strong chirality encourages entanglements and leads to broad distributions. We also examine the windings of flux lines in the presence of point impurities (random bonds). Our results suggest that pinning to impurities reduces entanglements, leading to a narrow (Gaussian) distribution. [S1063-651X(96)10606-1]

PACS number(s): 02.50.−r, 05.40.+j, 74.60.Ge

I. INTRODUCTION AND SUMMARY

Winding angles of paths are of great interest not only in mathematics, but also in the physics of polymers, and flux lines in high-T_c superconductors. The topological constraints produced by the windings of polymers [1] or magnetic flux lines [2,3] around each other result in entangled phases with slow dynamics. The simplest case that can be studied is the winding of a two-dimensional random walk around a point, or equivalently, a flux line in three dimensions around a columnar pin [4]. In 1958, Spitzer [5] showed that the probability distribution for the winding angle θ of a Brownian path around a point is a Cauchy law for large time t, i.e.,

$$\lim_{t\to\infty} p\left(x=\frac{2\theta}{\ln t}\right)=\frac{1}{\pi}\,\frac{1}{1+x^2}. \tag{1}$$

Similar Cauchy laws are obtained for winding around several points in two dimensions [6], and around several straight lines in three dimensions [7]. These results are obtained by employing a variety of techniques such as standard diffusion equation [5,8–10], path integrals [10,11], or probability theory [12,6,7]. By contrast, the winding angle of a self-avoiding walk in two dimensions obeys a Gaussian distribution, the scaling variable being $x=\theta/\sqrt{4\ \ln t}$ [13,14]. (See also Ref. [15] for an expansion around four dimensions.)

As pointed out in Refs. [16,17], the above Cauchy law has pathological properties that make its relevance to any physical situation questionable. In particular, because of the slowly decaying tails at large x, the averages of both θ^2 and $|\theta|$ are infinite. The origin of this divergence is that a finite segment of the Brownian walk can wind infinitely often around a point center. While this is correct for an idealized random walk, in any physical system one expects a cutoff due to either finite diameters or stiffness. The case of a Brownian walk in two dimensions around a disk of finite diameter was studied in Ref. [16]. The resulting winding angle distribution is [16,18]

$$\lim_{t\to\infty} p_A\left(x=\frac{2\theta}{\ln t}\right)=\frac{\pi}{4\ \cosh^2(\pi x/2)}. \tag{2}$$

In Ref. [17], the following result for the winding angle distribution for a random walk with steps of finite size is derived:

$$\lim_{t\to\infty} p_R\left(x=\frac{2\theta}{\ln t}\right)=\frac{1}{2}\,\frac{1}{\cosh(\pi x/2)}. \tag{3}$$

The same result is obtained in Ref. [6] for the distribution of ''big windings'' of Brownian motion around two pointlike winding centers. The relation between ''big'' and ''small'' windings is discussed in detail in [8]. Saleur [18] suggests that the difference between Eqs. (2) and (3) is due to different boundary conditions for the walkers at the winding center. A review of many topological and entanglement properties of polymers can be found in Ref. [19].

In this paper, we further study the issue of winding angle distributions and their universality, with particular emphasis on their applicability to magnetic flux lines (FLs) in high-T_c superconductors. We start in Sec. II by providing a derivation of Eqs. (1)–(3) based on conformal properties of random walks that do not require any advanced mathematical techniques. Although these equations have been known for some time, the difference between Eqs. (2) and (3) seems to have never been pointed out, except for the above-mentioned remark in Ref. [18]. Our derivation illustrates well the origin and universality of the exponential tail in Eqs. (2) and (3), and explains the factor 2 between their two decay constants. We argue that these two cases are applicable respectively to the windings of a flux line around a repulsive or marginal columnar defect. Actually, most columnar defects are attractive and localize the flux line to their vicinity. The corresponding probability distributions (for walkers with initial and final points close to the winding center) are also calculated in Sec. II D.

To test the generality of the analytical results, we performed a number of numerical tests that are described in Sec. III. Simulations of random walks were performed on both square and cubic lattices. For reflecting boundary conditions we chose a winding center that was shifted from the lattice sites crossed by the walker. For absorbing boundary conditions, the center was one of the lattice sites that the walkers

were not allowed to cross. A transfer matrix method can be used to evolve the winding angle distribution with the number of steps t. Despite a rather slow convergence to the asymptotic limit, the numerical results do indeed support the universality of distributions given in Eqs. (2) and (3).

In the course of numerical tests, we encountered one case (reflecting boundary conditions for a directed path along the diagonal of a cubic lattice) that did not conform to any of the above expected universality classes. Further examination revealed that we had inadvertently constructed a *chiral defect*: upon encountering the defect, the path had a statistical advantage to wind in one direction as opposed to the other. In the language of random walks, this corresponds to a rotating winding center. The breaking of the symmetry at the center is in fact a relevant perturbation, and leads to the probability distribution discussed in Sec. IV. Although we do not yet have a complete analytic understanding of this universality class, we can account for certain features of this distribution. In particular, weak chirality leads to narrow asymmetric distributions, while for strong chirality both wings of the distribution are widened, i.e., strong chirality of the defect enhances entanglements.

All the distributions examined in Secs. II–IV describe the windings of *ideal* random walks, and in all cases the appropriate scaling variable is the combination $x=2\theta/\ln t$. This universal feature is due to the *Markovian* nature of these walks, and can be explained as follows: After time t, the walker has a typical distance $r(t)\propto\sqrt{t}$ from the starting point, which is chosen to be close to the winding center. Assuming that $r(t)$ is the only relevant length scale, dimensional arguments, combined with the Markovian property, suggest that $dr/d\theta=rf(\theta)$. The rotational invariance of the system implies that $f(\theta)$ must be a constant; i.e., the increase in winding angle cannot depend on the number of windings or angular position. Hence,

$$d\theta\propto\frac{dr}{r}\propto\frac{dt}{t}=d(\ln t), \tag{4}$$

leading to a scaling variable proportional to $\theta/\ln t$.

Because of their non-Markovian nature, we cannot apply the arguments of the preceding paragraph to *self-avoiding walks*. Indeed, such walks have a Gaussian winding angle distribution in the scaling variable $x=\theta/\sqrt{\ln t}$ [13,14]. The self-similarity of the walk suggests the following scaling argument: Starting from the origin, divide the walk into segments of 1, 2, $\ldots,2^n\approx t/2$ steps. Since the αth segment is at a distance of roughly $2^{\alpha\nu}$ from the center (with $\nu=3/4$) and has a characteristic size of the same order, it is reasonable to assume that each segment spans a random angle θ_α of order one. Under the mild assumption that the sum $\theta=\Sigma_{\alpha=1}^{n}\theta_\alpha$ satisfies the central limit theorem, we then conclude that θ is Gaussian distributed with a variance proportional to $n\propto\ln t$. Similar scaling arguments, suggesting a scaling variable $x=\theta/\sqrt{\ln t}$ for self-avoiding walks, and $x=\theta/\ln t$ for ideal walks were first given in Ref. [13].

We can ask why the above argument of self-similarity does not apply to ideal walks. The reason is the relevance of the finite winding center. An important difference between ideal and self-avoiding walks is that the probability of returning to the winding center at the origin asymptotically vanishes for the latter because of the exclusion zone set up by self-avoidance. It is thus expected that properties of the winding center (size, absorbing versus reflecting nature, chirality) are irrelevant for self-avoiding walks. The ideal walks, on the other hand, return to the origin quite often, and upon rescaling see winding centers of different size. The assumption that different scaled portions of the ideal walk are self-similar is not correct.

There is one case where both arguments should hold: An ideal walk around a point winding center. The argument based on self-similarity actually states that the final distribution is obtained from the composition of $\ln t$ independent random variables. If each variable has a finite variance, the overall distribution will be Gaussian. If not, other (Levy) distributions are possible. The Cauchy distribution is in fact a limiting case for widely distributed variables. The requirement that both arguments should hold immediately selects a Cauchy distribution.

The scaling argument, which by no means is claimed to be exact, should apply to other self-similar walks where the probability of return to the origin is small. An interesting example is provided by directed paths in random media [20], which, for example, describe the behavior of a flux line in the presence of (quenched) point impurities. Typical wanderings of such paths scale as t^ν, with $\nu\approx0.62>1/2$. The pinning by impurities greatly reduces the probability of the walker returning to the origin, and the above arguments again suggest that the winding angle distribution is Gaussian. Although certainly not conclusive, the numerical results reported in Sec. V appear to support this prediction. Typical winding angles thus scale as $\sqrt{\ln t}$ as opposed to $\ln t$ in the pure case. This simple example thus suggests that topological entanglements become relatively less important in the presence of pinning to impurities.

The results of this paper point out the rich behavior already present in the simplest of problems involving topological defects. Properties of the winding center (finite size, chirality, etc.), interactions, and various types of randomness are all potentially relevant, leading to different universal distribution functions. These results could also produce some interesting physical manifestations. For example, we demonstrate in Sec. VI that there is a sharp crossover between free and coiled configurations if there is an energy proportional to the winding number.

II. DERIVATION OF WINDING ANGLE DISTRIBUTIONS

A. Spitzer's law

Before studying the winding of a Brownian path around a center of finite diameter, we first sketch a derivation of Spitzer's law in Eq. (1). We follow the approach in Ref. [12], translating it into a more physical language that does not rely on a familiarity with martingales. A basic ingredient is the invariance of Brownian motion under conformal mappings. Let

$$z(t)=x_1(t)+ix_2(t) \tag{5}$$

represent the original walk in the complex two-dimensional plane. The time evolution of each random walker satisfies

$$dz=\eta(t)dt, \tag{6}$$

where the complex random velocity has zero mean and is uncorrelated at different times, with

$$\langle \eta(t)\,\eta^*(t')\rangle = 2D\,\delta(t-t'). \tag{7}$$

The radius of the walker and its winding angle can be extracted from

$$\zeta(t)=\ln z(t)=\rho(t)+i\,\theta(t), \tag{8}$$

where $\rho=\ln r=\ln\sqrt{x_1^2+x_2^2}$. Since $d\zeta=\eta(t)dt/z(t)$, the stochastic motion of the walker in the new complex plane is highly correlated to its location. This feature can be removed by defining a new time variable

$$d\tau=\frac{dt}{|z(t)|^2} \tag{9}$$

for each walker, which leads to

$$d\zeta=\mu(\tau)d\tau, \text{ with } \mu(\tau)=z^*(t)\,\eta(t). \tag{10}$$

Since

$$\langle \mu(\tau)\mu^*(\tau')\rangle = 2D|z(t)|^2\delta(t-t')=2D\,\delta(\tau-\tau'), \tag{11}$$

the evolution of $\zeta(\tau)$ is that of a Brownian walk.

For simplicity we choose the initial condition $\zeta(t=\tau=0)=0$; i.e. the original walker starts out at $z=1$. We also set the diffusion constant to $D=1/2$, so that the mean square distance over which the walk moves during a time t is $\langle r^2(t)\rangle = t$. The probability that $r(t)$ is within an interval $[\sqrt{\pi}t^{(1-\epsilon)/2},\sqrt{\pi}t^{(1+\epsilon)/2}]$ around its mean value of $\sqrt{\pi}t$,

$$p(t,\epsilon)=\int_{\sqrt{\pi}t^{(1-\epsilon)/2}}^{\sqrt{\pi}t^{(1+\epsilon)/2}}\frac{\exp(-r^2/2t)}{2\pi t}2\pi r\,dr$$

$$=\int_{\pi t^{-\epsilon/2}}^{\pi t^{\epsilon/2}}\exp(-s)ds, \tag{12}$$

approaches unity in the limit $t\to\infty$. In this limit, the distance r from the starting point $z=1$ is identical to the distance from the origin, and $p(t,\epsilon)$ is identical to the probability that $\zeta(\tau)$ is in the interval $[0.5(1-\epsilon)\ln t, 0.5(1+\epsilon)\ln t]$. If we shrink the complex plane ζ by a factor of $(\ln t)/2$, the walker is within a distance ϵ of the line with a real value of unity. Thus, all walks of length t in the z plane are mapped on walks that hit the line with a real value of unity for the first time. Since there is a separate transformation $\tau(t)$ for each walker, walks of the same length t map on walks of different length τ. (To be precise, we also have to shrink the time scale τ when shrinking the ζ plane, but for simplicity we denote the new time again by τ.)

The imaginary coordinate x of the hit is now related to the winding angle by $x=2\,\theta(t)/\ln t$. Thus, in the limit $t\to\infty$, the probability $p(x)dx$ is precisely the probability that a Brownian walker $(2\zeta/\ln t)$ starting from the origin hits a vertical line at a distance one from the origin, for the first time, at a height between x and $x+dx$. We therefore need the probability density $p_1(\tau)$ that the first hit is at τ. Its integral $P_1(\tau)=\int_0^\tau d\tau' p_1(\tau')$ is the probability for the walker to hit the line at least once before time τ. Since after hitting the wall the walker is equally likely to proceed in either direction, the latter is also twice the probability that the end point of the walk is beyond the line at τ, and hence given by

$$P_1(\tau)=2\int_1^\infty\frac{\exp(-r^2/2\tau)}{\sqrt{2\pi\tau}}dr=\int_0^\tau\frac{\exp(-1/2s)}{\sqrt{2\pi s^3}}ds.$$

The derivative gives

$$p_1(\tau)=\frac{dP_1}{d\tau}=\frac{1}{\sqrt{2\pi\tau^3}}\exp\left(-\frac{1}{2\tau}\right).$$

Since the vertical and horizontal components of the walk are independent, we finally obtain

$$p(x)=\int_0^\infty d\tau\frac{\exp(-1/2\tau)}{\sqrt{2\pi\tau^3}}\frac{\exp(-x^2/2\tau)}{\sqrt{2\pi\tau}}=\frac{1}{\pi}\frac{1}{1+x^2},$$

which is Spitzer's law, exact in the limit $t\to\infty$.

B. Repulsive defects and finite absorbing centers

The unphysical situation that a path element of finite length can wind infinitely often around the origin can be removed by introducing a winding center of finite size. A FL winding around a repulsive columnar defect cannot penetrate the defect, and all configurations where the FL and the defect intersect have to be removed [16]. This situation corresponds to a random walk around an absorbing winding center. Two directed polymers with hard-core interaction winding around each other are described by the same situation, the radius r now being the relative distance between the two polymers.

We choose a disk of radius $R<1$ around the origin, which cannot be entered by the Brownian walk $z(t)$. A path of length t now has a maximum winding angle of t/R. The walk is again started from $z(0)=1$, and after a long time t, its end point is almost certainly at a distance r between $\sqrt{\pi}t^{(1-\epsilon)/2}$ and $\sqrt{\pi}t^{(1+\epsilon)/2}$ from the origin, as given by Eq. (12). (The excluded disk of radius $R\ll\sqrt{t}$ has negligible influence in this limit.) The random walks in the complex plane $\zeta=\ln z$ consequently have real values in the interval $[0.5(1-\epsilon)\ln t, 0.5(1+\epsilon)\ln t]$ as before. But now the walks $\zeta(\tau)$ cannot go to the left of a line at $a=\ln R$. The probability density $p_A(x)$ for having a scaled winding angle $x=2\,\theta/\ln t$ is therefore identical to the probability density that a random walk starting at the origin hits a line at distance one, for the first time, at height x without going beyond a line at distance $2|\ln R|/\ln t$ on the opposite side.

Let $P_{a,b}(y,\tau)$ denote the probability that a Brownian walk starting at $y\in[a,b]$ hits the point b for the first time during a time interval τ, without hitting point a previously. If we consider the points a and b as absorbing boundaries, this is identical to the probability that the walk is absorbed at boundary b before time τ. Since for sufficiently small $\Delta\tau$, the walker is only a short distance Δy from its starting point, we have

$$P_{a,b}(y,\tau)=\int_0^\infty d(\Delta y)\,\frac{1}{\sqrt{2\pi\Delta\tau}}\exp\left[-\frac{(\Delta y)^2}{2\Delta\tau}\right]\times[P_{a,b}(y+\Delta y,\tau-\Delta\tau)+P_{a,b}(y-\Delta y,\tau-\Delta\tau)].$$

Expanding the above equation to the order of Δt indicates that $P_{a,b}(y,\tau)$ satisfies a diffusion equation. The appropriate boundary conditions are $P_{a,b}(a,\tau)=0$ and $P_{a,b}(b,\tau)=1$ with the initial value $P_{a,b}(y,0)=0$, resulting in [21]

$$P_{a,b}(y,\tau)=\frac{y-a}{b-a}+\frac{2}{\pi}\sum_{\nu=1}^{\infty}\frac{(-1)^{\nu+1}}{\nu}\sin\left(\frac{\pi\nu(y-a)}{b-a}\right)\times\exp\left[-\frac{1}{2}\left(\frac{\pi\nu}{b-a}\right)^2\tau\right].$$

The probability that the walk is absorbed at the right-hand boundary during the time interval $[\tau,\tau+d\tau]$ is $d\tau\partial_\tau P_{a,b}(y,\tau)$. Note, however, that $\int_0^\infty d\tau\partial_\tau P_{a,b}(y,\tau)=(y-a)/(b-a)$, i.e., equal to the total fraction of particles absorbed at the right-hand boundary (inversely proportional to the separations from the boundaries). To calculate $p_A(x)$, we need the fraction of these walks absorbed between τ and $\tau+d\tau$, equal to $[(b-a)/(y-a)]\partial_\tau P$. Hence (with $a=2\ \ln R/\ln t$, $b=1$ and $y=0$)

$$p_A(x)=\int_0^\infty d\tau\frac{1-a}{-a}\,\frac{\partial P_{a,1}(0,\tau)}{\partial\tau}\,\frac{\exp(-x^2/2\tau)}{\sqrt{2\pi\tau}}$$

$$=\int_0^\infty d\tau\sum_{\nu=1}^{\infty}\frac{(-1)^{\nu+1}}{\sqrt{2\pi\tau}}\,\frac{\pi\nu}{a(1-a)}\sin\left(\frac{\pi\nu a}{1-a}\right)\times\exp\left[-\frac{1}{2}\left(\frac{\pi\nu}{1-a}\right)^2\tau-\frac{x^2}{2\tau}\right]$$

$$=\sum_{\nu=1}^{\infty}\frac{(-1)^{\nu+1}}{a}\sin\left(\frac{\pi\nu a}{1-a}\right)\exp\left[-\frac{\pi\nu|x|}{(1-a)}\right].$$

The last step is achieved by first performing a Fourier transform with respect to x, followed by integrating over τ, and finally inverting the Fourier transform. (Alternatively, the τ integration can be performed by the saddle point method.) In the limit of large t, the variable a is very small, and we can replace the sine function by its argument. Taking the sum over ν, we find

$$p_A(x)=\frac{\pi}{1-a}\,\frac{\exp[\pi x/(1-a)]}{\{\exp[\pi x/(1-a)]+1\}^2}. \tag{13}$$

Changing the variable from x to

$$\tilde{x}=\frac{x}{(1-a)}=\frac{2\theta}{\ln(t/R^2)},$$

and noting that $p_A(x)dx=p_A(\tilde{x})d\tilde{x}$, leads from Eq. (13) to

$$p_A\left(\tilde{x}=\frac{2\theta}{\ln(t/R^2)}\right)=\frac{\pi}{4\,\cosh^2(\pi\tilde{x}/2)}. \tag{14}$$

This is identical to Eq. (2), since $\tilde{x}=x$ for large t. The use of the variable $\tilde{x}$ is, however, more appropriate, since it makes the argument of the logarithm dimensionless, and explicitly indicates the basic time unit. The above distribution, which is exact in the limit $t\to\infty$, has an exponential decay for large $\tilde{x}$, in contrast to Spitzer's law in Eq. (1). In particular, the mean winding angle is now finite. The analogy to random walkers in the plane ζ, confined by the two walls, provides simple physical justifications for the behavior of the winding angle. In the presence of both walls, the diffusing particle is confined to a strip, and loses any memory of its starting position at long times. The probability that a particle that has already traveled a distance θ in the vertical direction proceeds a further distance $d\theta$ without hitting either wall is thus independent of θ, leading to the exponential decay. On the other hand, if there is no confining wall on the left-hand side, the particles may diffuse arbitrarily far in that direction, making it less probable to hit the wall on the right hand side. The absence of a characteristic confining length thus leads to the unphysical divergence in Spitzer's law.

We also expect that different shapes of the winding center do not modify Eq. (14). This is because of the division by $\ln t/2$, which maps any excluded shape to the vertical line at $a=0$ for long enough times. However, different shapes should result in different effective values for R, and the time constant in Eq. (14). For long times, the polar angle of the particle may take any value between 0 and 2π with equal probability, and the particle sees an averaged radius of the winding center.

The crossover to Spitzer's law in the limit $R\to 0$ is not apparent from the above expression for $p_A(x)$. The transition can be made in the initial equation for $p_A(x)$, but not in the final result of Eq. (14), where time is measured in units of R^2. The time scale in Spitzer's law is set by the distance of the initial point from the winding center, which is infinite in units of the radius of the winding center. Consequently one time unit in Eq. (1) corresponds to infinitely many time units in Eq. (14), and the limits $t\to\infty$ or $R\to 0$ or $\tilde{x}\to 0$ in Eq. (14) correspond to the limit $t\to 0$ or $x\to\infty$ in Eq. (1).

C. Neutral defects and reflecting winding centers

For windings around several point centers, or the winding of a random walk on a lattice around a point different from the vertices of the lattice [6,17], no configurations are forbidden, and no walks are removed. The resulting winding angle distribution in both cases is given by Eq. (3). The random walk on a lattice can be regarded as a model for a directed polymer of finite stiffness, the step size being of the order of the persistence length. This situation applies to magnetic FLs winding around a columnar defect that is marginal, i.e., neither attractive nor repulsive. We can obtain Eq. (3) by repeating the calculations of the previous subsection, but replacing the absorbing boundary condition $P_{a,b}(a,\tau)=0$ with

the reflecting condition $\partial P_{a,b}(y,\tau)/\partial y|_{y=a}=0$. There is thus no current leaving the system at point a, and walkers that hit the winding center are reflected. We then find

$$P_{a,b}(y,\tau)=1-\frac{2}{\pi}\sum_{\nu=0}^{\infty}\frac{1}{\nu+1/2}\sin\left(\frac{\pi(\nu+1/2)(b-y)}{b-a}\right)\times\exp\left[-\frac{1}{2}\left(\frac{\pi(\nu+1/2)}{b-a}\right)^2\tau\right] \quad (15)$$

and

$$\begin{aligned}p_R(x)&=\int_0^\infty d\tau\frac{\partial P_{a,1}(0,\tau)}{\partial\tau}\frac{\exp(-x^2/2\tau)}{\sqrt{2\pi\tau}}\\&=\sum_{\nu=0}^{\infty}\frac{1}{1-a}\sin\left(\frac{\pi(\nu+1/2)}{1-a}\right)\times\exp\left[-\frac{\pi(\nu+1/2)|x|}{(1-a)}\right]\\&=\frac{1}{2(1-a)\cosh(\pi x/2)},\end{aligned}$$

or, equivalently,

$$p_R(\tilde{x})=\frac{1}{2\cosh(\pi\tilde{x}/2)}, \quad (16)$$

where again time is measured in units of R^2, and the limit $t\to\infty$ has been taken. For large $\tilde{x}$, where the walk has lost the memory of its initial distance from both walls, this probability decays exponentially as $\exp(-\pi\tilde{x}/2)$. A random walk confined between an absorbing and a reflecting wall that have a distance 1 can be mapped to a random walk confined between two absorbing walls at distance 2. After rescaling the wall distance and the $\tilde{x}$ coordinate by two, this explains the factor 1/2 between the decay constants in the tails of the distributions in Eqs. (2) and (3).

D. Attractive defects and returning walks

A magnetic FL winding around an attractive columnar defect of radius b_0 and binding energy U_0 per unit length is bound to that defect. If the temperature is above a crossover temperature $T^*\propto b_0\sqrt{U_0}$, the line is only weakly bound and wanders horizontally over the distance of the localization length $l_\perp(T)\simeq b_0\exp[(T/T^*)^2]$ [4]. The mean vertical distance l_z between consecutive intersections of the FL with the defect is consequently proportional to $l_\perp^2$. Over this distance the FL can be approximated by a directed walk, which returns to its starting point (the winding center) after a time l_z.

Using the result in Eq. (14), we can derive the winding angle distribution $p_A^o(\tilde{x})$ for such confined random walks. Each walk that returns to its starting point after time t (in the z plane) is composed of two walks of length $t/2$ going from the starting point to $z(t/2)$. As we have seen in Sec. II A, almost all walks of length $t/2$, when mapped on the plane $2\zeta/\ln(t/2)$, have their end point on a vertical wall at distance 1 from the origin. The winding angle distribution for these walks is given by Eq. (14), with t replaced by $t/2$. The probability that a walk that returns to its starting point has a winding angle θ is therefore obtained by adding the probabilities of all combinations of two walks of length $t/2$ whose winding angles add up to θ, i.e.,

$$\begin{aligned}p_A^o(\tilde{x})&=\int_{-\infty}^{\infty}dy\frac{\pi}{4\cosh^2(\pi y)}\frac{\pi}{4\cosh^2[\pi(\tilde{x}-y)]}\\&=\frac{\pi}{2\sinh^2(\pi\tilde{x}/2)}\left(\frac{\pi\tilde{x}}{2}\coth\left(\frac{\pi\tilde{x}}{2}\right)-1\right),\end{aligned} \quad (17)$$

where $\tilde{x}=2\theta/\ln(t/2R^2)$. Surprisingly, this result is different from the one given in Eq. (4.1) of Ref. [18]. We are not sure of the origin of this discrepancy, but note that the result in Ref. [18] has a divergence at $\tilde{x}=0$ that is unphysical.

If in place of convoluting two absorbing probability distributions, as in Eq. (17), we use the probability distributions for reflecting boundary conditions, the final result is modified to

$$p_R^o(\tilde{x})=\frac{\tilde{x}}{2}\frac{1}{\sinh(\pi\tilde{x}/2)}. \quad (18)$$

For large $\tilde{x}\approx x$, the above two expressions decay as $x\exp(-\pi x)$ and $x\exp(-\pi x/2)$, respectively. A FL of length L is broken up into roughly L/l_z segments between contacts with the attractive columnar defect. We can assume that the winding angle of each segment is independently taken from the probability distribution in Eq. (17) with $t\approx l_z$. Adding the winding angle distributions of all segments leads to a Gaussian distribution centered around $\theta=0$, and with a variance proportional to $L\ln(l_z)/l_z$. Similar Gaussian distributions are also obtained for diffusion confined to a disk of finite radius [22].

III. UNIVERSALITY OF THE WINDING ANGLE DISTRIBUTION

At first sight it may seem surprising that the winding angle distribution in Eq. (16) for random walks around a reflecting center of finite diameter is identical to the distribution of ''large windings'' for Brownian motion around two pointlike centers [6], or to distribution for random walks of finite step size [17]. The increase in winding angle is largest when the walk is close to the winding center, and should thus be quite sensitive to the lattice structure, or the ratio between step size and winding center size. However, a closer examination of the random walks in the scaled ζ plane reveals that, in the limit $t\to\infty$, almost no increase in the variable $\tilde{x}$ occurs when the walker is within a certain finite distance from the winding center (corresponding to an infinitely small distance from the reflecting wall in the scaled ζ plane). A similar conclusion was reached in Ref. [8], where the two-dimensional plane is divided into three concentric regions. It is shown that the contribution of the middle region to the winding angle scales as $\sqrt{\ln t}$, compared to a contribution proportional to $\ln t$ in the outer region. Hence, microscopic details do not enter the winding angle distribution, and Eq. (16) holds as long as there is a winding center of nonvanishing size (or, equivalently, an upper cutoff to the

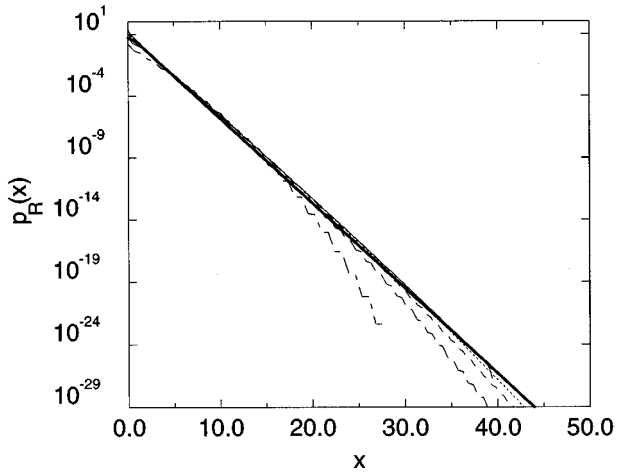

FIG. 1. Winding angle distribution for random walks on a square lattice with *reflecting* boundary conditions for $t=38$ (dot-dashed), 152 (long dashed), 608 (dashed), 2432 (dotted), and 9728 (solid). The horizontal axis is $x=2\theta/\ln(2t)$. The thick solid line is the analytical result of Eq. (3).

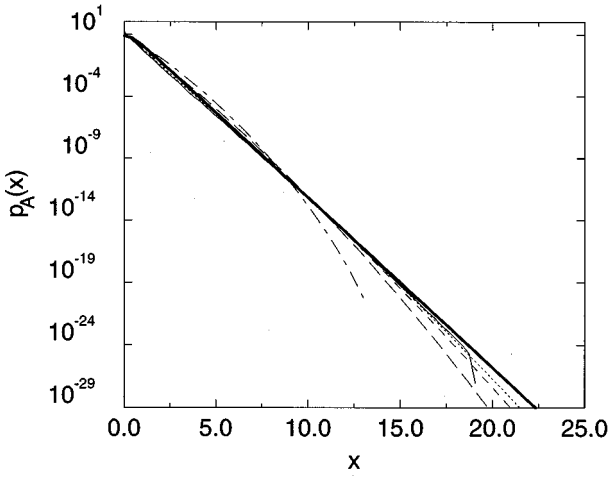

FIG. 2. Winding angle distribution for random walks on a square lattice with *absorbing* boundary conditions. The symbols and the variable x are the same as in the previous figure. The thick solid line is the analytical result of Eq. (2).

maximum possible winding angle per unit time), and as long as no walk coming close to the winding center is absorbed.

If a walk hitting the winding center is absorbed with a nonvanishing probability, almost all walks are absorbed in the limit $t\to\infty$, and the winding angle distribution of the surviving walks is given by Eq. (14). As for reflecting boundary conditions, microscopic details of the system do not influence this distribution. Apart from these two universality classes, we shall later encounter a third class of walks corresponding to random motion around a rotating winding center; the winding angle distribution in this case depends on the rotation speed of the center. In this section, we check numerically the former situations, where the symmetry between $\pm\theta$ is not broken.

We performed computer simulations of random walks on a square lattice with both reflecting and absorbing boundary conditions. Reflecting boundary conditions are simply realized by choosing a winding center different from the vertices of the lattice, and thus never crossed by the walker. On the other hand, to simulate absorbing boundary conditions, the winding center is chosen as one of the lattice sites (say the origin), but no walk is allowed to go through this point.

The winding angle distributions are most readily obtained using a transfer matrix method that calculates the number of all walks with given winding angle and given end point after t steps, from the same information after $t-1$ steps. The winding center is at (0.5,0.5) for reflecting boundary conditions, and at the origin for absorbing boundary conditions. The walker starts at (1,0), and the winding angle is increased or decreased by 2π every time it crosses the positive branch of the x_1 axis. Due to limitations in computer memory, we applied a cutoff in system size and winding angle for times $t>120$, making sure that the results are not affected by this approximation. The largest times used, $t=9728$, required approximately 3 days to run on a Silicon Graphics Indy Workstation.

Figures 1 and 2 show the simulation results for the two cases. The asymptotic exponential tails predicted by theory can clearly be seen; deviations from the theoretical curve for smaller values of the scaling variable $x=2\theta/\ln(2t)$ are due to the slow convergence to the asymptotic limit. Since the scaling variable depends logarithmically on time, the asymptotic limit is reached only for large ln$t$. Note that the only free parameter in fitting to the analytical form is the characteristic time scale appearing inside the logarithm. With t measured in units of single steps on the lattice, we found that a factor 2 in the scaling variable provides the best fit. In the limit $t\to\infty$, different scales of t give of course the same asymptotic winding angle distribution.

To further test the universality of these distributions, we also performed simulations of a flux line (directed path) proceeding along the diagonal of a cubic lattice in three dimensions. The FL starts at (1,0,0), and at each step increases one of its three coordinates by 1. We determined the winding angle distribution around the diagonal (1,1,1) direction, excluding from the walk all points that are on this diagonal (a repulsive columnar defect, corresponding to the case of an absorbing winding center). The excluded points lie on the origin when the FL is projected in a plane perpendicular the diagonal. A cutoff of 243 in system size was imposed for the transfer matrix calculations. The winding angle distribution $p(x=2\theta/\ln t)$ is shown in Fig. 3 for different times. As for the square lattice, an exponential tail with a decay constant of π can be seen clearly. Our numerical results, as well as the analytical considerations, thus indicate clearly that the winding angle distributions for reflecting and absorbing boundary conditions are universal and do not depend on microscopic details.

Due to the special properties of directed paths along the diagonal of the cube, the case of reflecting boundary conditions leads to an asymmetry between windings in positive and negative directions. This is because it takes only three steps to make the smallest possible winding in one direction, but six steps in the opposite direction. This situation is discussed in detail in Sec. IV.

IV. CHIRAL DEFECTS AND ROTATING WINDING CENTERS

So far, we have only considered situations that are symmetric with respect to the angles $\pm\theta$. For directed paths on

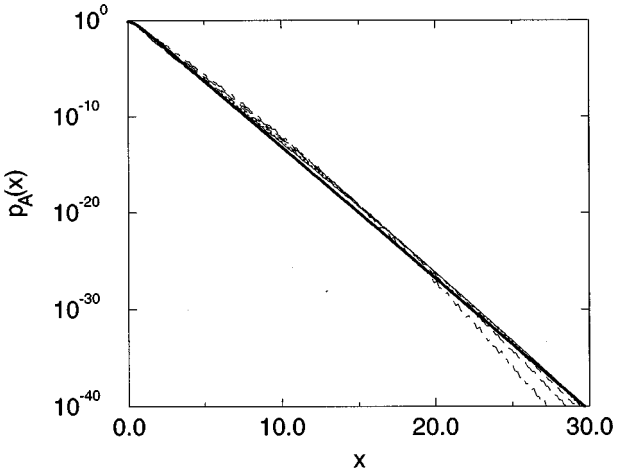

FIG. 3. Winding angle distribution around the preferred direction for a flux line (directed path) in three dimensions for $t=243$ (dot-dashed), 729 (long dashed), 2187 (dashed), 6561 (dotted), and 19 684 (solid). The horizontal axis is $x=2\theta/\ln(2t)$. The thick solid line is the analytical result of Eq. (2).

certain lattices, however, this symmetry is broken, as mentioned in Sec. III. A directed walk that proceeds at each step along the $+x_1$, $+x_2$, or $+x_3$ direction on a cubic lattice can be mapped on a random walker on a two-dimensional triangular lattice as indicated in Fig. 4(a). Each bond can be crossed in only one direction, and the winding center for reflecting boundary conditions must be different from the vertices of the lattice. It is apparent from this figure that the random walker can go around the center in three steps in one angular direction, but in no less than six steps in the other direction.

An alternative description is obtained by examining the position of the walker after every three time steps. The resulting coarse-grained random walk takes place on a regular triangular lattice, but now the walker has a finite probability of $3\times 2/3^3=2/9$ of staying at the same site. If this site is one of the three points next to the winding center, the winding angle is increased by 2π in one of the six possible configurations that return to the site after three steps. In other words, the walker has a finite probability of having its winding angle increased in the proximity of the center. The amount of this biased increase in angle depends on the structure of the lattice and will be different for other directed lattices. An equivalent physical situation occurs for Brownian motion around a rotating winding center, e.g., a rotating reflecting disk that does not set the surrounding gas or liquid into motion.

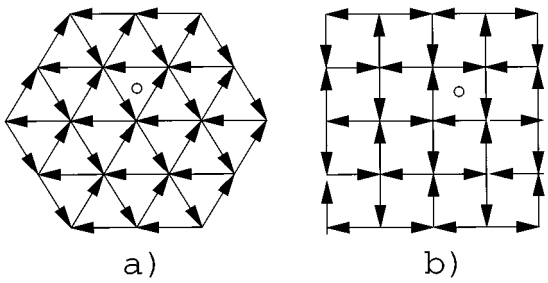

FIG. 4. Triangular and square lattices with directed bonds. The winding centers are indicated by the open circle.

Since this angular symmetry breaking is already present in the above simple example of a directed walk, it is also likely to occur in more realistic physical systems, such as with screw dislocations. We thus use the term *chiral* columnar defect to indicate that each time the FL comes close to the defect, it finds it easier to wind around in one direction as opposed to the other. (Of course, to respect the reflecting boundary conditions, there must be no additional interaction with the defect.) After mapping to the rescaled ζ plane introduced in Sec. II, the above situations can be modeled by an upward moving reflecting wall on the vertical axis. Each time a Brownian walker hits this wall, its vertical position $x=2\theta/\ln t$ is increased by a small amount $2\Delta\theta/\ln t$. Let us now determine the net shift Δx in x due to the motion of the wall for a walker that survives for a time τ in the rescaled ζ plane, before it is absorbed at the right-hand wall (recall that t is the time in the original system, while τ refers to the time in the rescaled ζ plane, after the conformal mapping).

To obtain the full solution, it is necessary to solve the two-dimensional diffusion equation with moving boundary conditions. Since we are mainly interested in the exponential tails of the winding angle distribution, we restrict our analysis to the limit of large times τ, and determine the shift in x due to encounters with the reflecting moving wall in this limit. A Brownian walker that has survived for a sufficiently long time τ forgets its initial horizontal position. The mean number of encounters with the reflecting wall, and consequently the shift Δx in x due to the motion of the wall, is then expected to be simply proportional to the considered time interval. Assuming the validity of the central limit theorem in the limit $\tau\to\infty$, the probability distribution of Δx is given by

$$p_\Delta(\Delta x)=\frac{1}{\sqrt{2\pi\beta^2\tau}}\exp\left[-\frac{(\Delta x-\alpha\tau)^2}{2\beta^2\tau}\right]. \tag{19}$$

The parameters α and β are related to the velocity of the wall (chirality of the defect) by $\alpha\propto\beta\propto v$. Presumably Eq. (19) can be obtained directly from properties of random walks, providing the exact coefficients in the above proportionality.

We can now modify Eq. (16) to

$$\begin{aligned} p_R^c(x)&=\int_0^\infty d\tau\int_{-\infty}^{\infty}d(\Delta x)p_\Delta(\Delta x)\frac{\partial P_{a,1}(0,\tau)}{\partial\tau}\\ &\quad\times\frac{1}{\sqrt{2\pi\tau}}\exp\left[-\frac{(x-\Delta x)^2}{2\tau}\right]\\ &=\int_0^\infty d\tau\frac{\partial P_{a,1}(0,\tau)}{\partial\tau}\\ &\quad\times\frac{1}{\sqrt{2\pi\tau(1+\beta^2)}}\exp\left[-\frac{(x-\alpha\tau)^2}{2\tau(1+\beta^2)}\right]. \end{aligned}$$

In the limit of large x it is sufficient to take the first term in the series expansion for $P_{a,1}(0,\tau)$ given in Eq. (15), leading to

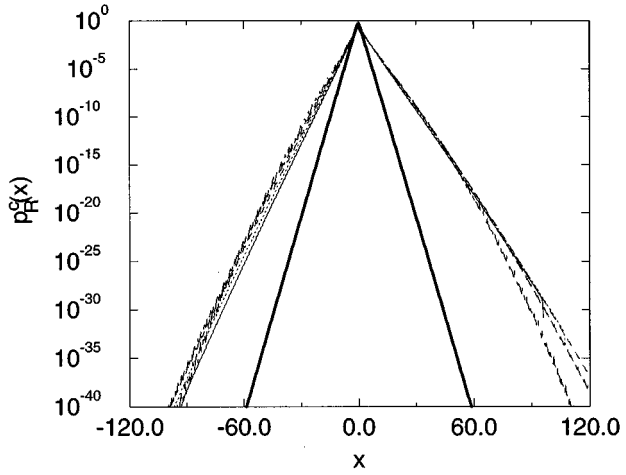

FIG. 5. Winding angle distribution around the preferred direction for a random walk on a directed triangular lattice for $t=243$ (dot-dashed), 729 (long dashed), 2187 (dashed), 6561 (dotted), and 19 684 (solid). The scaling variable is $x=2\theta/\ln(2t)$. The thick solid line is the distribution given in Eq. (3).

$$p_R^c(x)=\exp\left[\frac{\alpha x}{1+\beta^2}-\frac{|x|}{1+\beta^2}\sqrt{\alpha^2+\frac{\pi^2}{4}(1+\beta^2)}\right], \tag{20}$$

valid for large $|x|$. The effect of the moving wall on the winding angle distribution is thus a systematic shift in the slopes of the exponential tails. For small values of chirality the slopes on the two sides are changed to $\pi/2\pm\alpha$. Due to the velocity dependence, these asymmetric distributions are clearly nonuniversal. At large chiralities the slopes vanish as α/β^2, resulting in quite wide distributions. Apparently strong chirality of a defect increases the probability of entanglements. The scaling variable is $x=2\theta/\ln(2t)$. The thick solid line is the distribution Eq. (3).

Figure 5 shows our simulation results for the winding angle distribution for a walk on the above mentioned directed triangular lattice. The asymmetry due to the shift is clearly visible, and the winding angle distribution is wider than for a stationary wall. This case thus exemplifies the strong chirality limit discussed in the previous paragraph. We also simulated a square lattice with directed bonds as indicated in Fig. 4(b). The corresponding winding angle distribution is shown in Fig. 6. The distribution is again asymmetric, but not as wide as in the previous one, and more similar to that expected in the weak chirality regime.

A somewhat different situation is discussed in Ref. [24], where the winding of a polymer around an attractive and chirally asymmetric rod is studied. Below the localization temperature, the polymer is bound to the rod and has a finite mean winding angle proportional to its length. Above the localization temperature, the chirality has no effect at all on the winding angle, due to the hard-core repulsion at short distances, a situation that corresponds to absorbing boundary conditions. We expect that the reflecting boundary conditions discussed in this section may be relevant near the localization temperature.

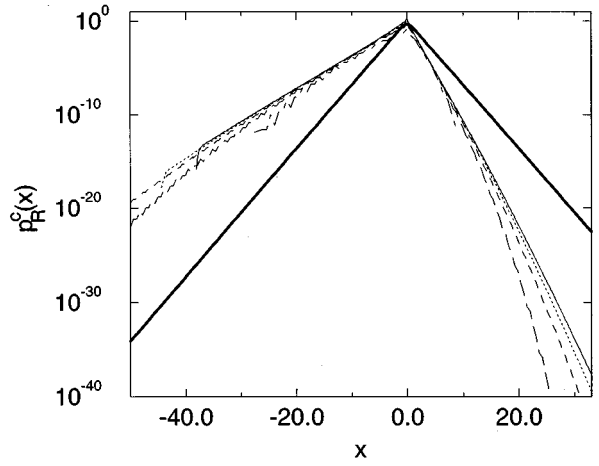

FIG. 6. Winding angle distribution for a random walk on a directed square lattice for $t=38$ (dot-dashed), 152 (long dashed), 608 (dashed), 2432 (dotted), and 9728 (solid).

V. WINDING ANGLES IN RANDOM MEDIA

FLs in high-T_c superconductors are pinned by oxygen impurities. Such pinning is quite essential to enhancing the current carrying capacity of the superconductor in its mixed phase [23]. Actually, the pinning to the (quenched) random impurities fundamentally modifies the properties of FLs, leading to glassy phases. The simplest example is again a single FL as discussed in the previous section. The behavior of the FL in the presence of point impurities can be modeled by a directed path on a lattice with random bond energies [20]. In three or fewer dimensions, the line is always pinned at sufficiently long length scales. An important consequence of the pinning is that the path wanders away from the origin much more than a random walk, its transverse fluctuations scaling as t^{ν}, where $\nu\approx 0.62$ in three dimensions, and $\nu=2/3$ in two dimensions [25,26]. The probability of such paths returning to the winding center are thus greatly reduced, and the winding probability distribution is expected to change.

We examined numerically the windings of a directed path along the diagonal of a cubic lattice [see Fig. 4(a)]. To each bond of this lattice was assigned an energy randomly chosen between 0 and 1. Since the statistical properties of the pinned path are the same at finite and zero temperatures, we determined the winding angle of the path of minimal energy by a transfer matrix method. For each realization of randomness this method [20] finds the minimum energy of all paths terminating at different points, and with different winding numbers. This information is then updated from one time step to the next. From each realization we thus extract an optimal angle as a function of t. The probability distribution is then constructed by examining 2700 different realizations of randomness. To improve the statistics, we averaged over positive and negative winding angles.

The resulting distributions are shown in Figs. 7 and 8. The scaling variable in Fig. 8 is $2\theta/\ln t$ and the results are compared to Eq. (2), which is expected in the pure system. A much better fit is achieved with the scaling variable $x=\theta/2\sqrt{\ln t}$ as indicated in Fig. 7. This scaling form is motivated by that of self-avoiding walks, which in two dimen-

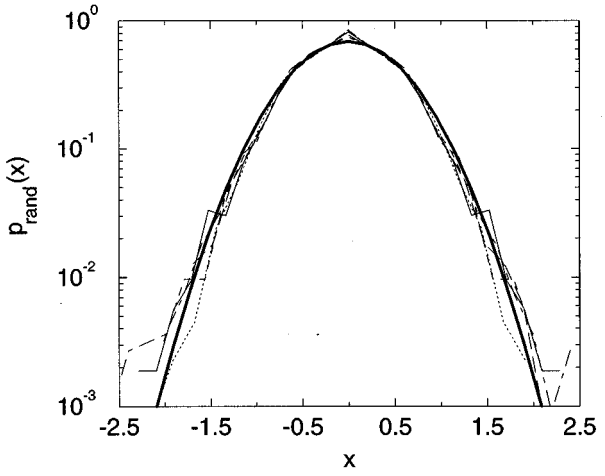

FIG. 7. Winding angle distribution for a directed path in a random three-dimensional system for $t=120$ (dotted), 240 (dashed), 480 (long dashed), 960 (dot-dashed), and 1920 (solid). The thick solid line is the Gaussian distribution in Eq. (22).

sions follow a Gaussian distribution

$$p_{\mathrm{SA}}\left(x=\frac{\theta}{2\sqrt{\ln t}}\right)=\frac{1}{\sqrt{\pi}}\exp(-x^2). \tag{21}$$

The result of the data collapse in Fig. 7 agrees well with the Gaussian distribution

$$p_{\mathrm{rand}}\left(x=\frac{\theta}{2\sqrt{\ln t}}\right)=\sqrt{\frac{1.5}{\pi}}\exp(-1.5x^2). \tag{22}$$

Directed paths in random media and self-avoiding walks share a number of features that make the similarity in their winding angle distribution plausible. Both walks meander away with an exponent larger than the random walk value of 1/2. (The exponent of 3/4 for self-avoiding walks is larger than $\nu\approx 0.62$ for FLs in three dimensions.) As a result, the probability of returns to the origin is vanishingly small in the $t\to\infty$ for both paths, and thus the properties of the winding center are expected to be irrelevant. [A simple scaling argument suggests that the number of returns to the origin scale as $N(t)\propto 1/t^{1-2\nu}$.] The conformal mapping of Sec. II cannot be applied in either case: The density and size of impurities in a random medium becomes coordinate dependent under this mapping, as does the excluded volume effect. The winding angle distribution for self-avoiding walks in Eq. (21) has been calculated using a more sophisticated mapping [14,18]. As a similar exact solution is not currently available for FLs in random media, we resort to the scaling argument presented next.

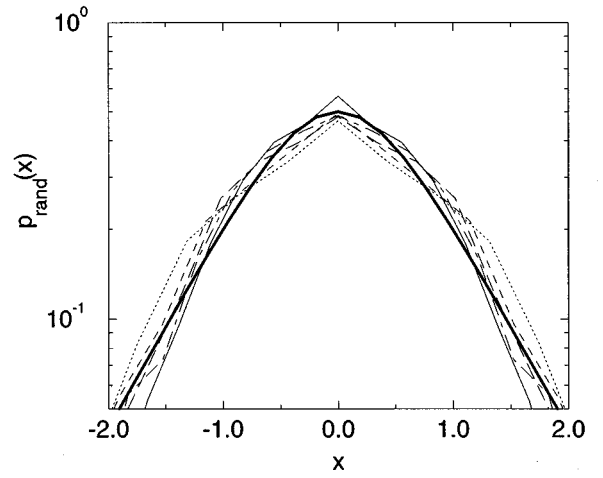

FIG. 8. Same distribution as in previous figure, but with $x=2\theta/\ln t$. The thick solid line is the distribution for the pure case given in Eq. (2).

Let us divide the self-avoiding walk, or the directed path, in segments going from $t/2$ to t, from $t/4$ to $t/2$, etc., down to some cutoff length of the order of the lattice spacing, resulting in a total number of segments of the order of $\ln t$. The statistical self-similarity of the walks suggests that a segment of length $t/2^n$ can be mapped onto a segment of length $t/2^{n+1}$ after rescaling by a factor of $1/2^{\nu}$. Under this rescaling, the winding angle is (statistically speaking) conserved, and consequently all segments have the same winding angle distribution. Convoluting the winding angle distributions of all segments, and assuming that the correlations between segments do not invalidate the applicability of the central limit theorem, leads to a Gaussian distribution with a width proportional to $\ln t$. This argument does not work for the random walks considered in Secs. II B–II D, since the finite radius of the winding center is a relevant parameter. Different segments of the walk are therefore not statistically equivalent, as they see a winding center of different radius after rescaling.

Another interesting quantitity to study is the difference in free energy between configurations of different winding numbers. This provides an estimate of the free energy that can be gained (or lost) by a FL upon changing its degree of entanglement. In the pure system, this quantity can be obtained directly from the winding angle distribution. For large t, the difference in free energy between configurations of winding number n and 0 is calculated by expanding Eq. (2) for small $x=4\pi n/\ln t$, and is given by

$$F(n)-F(0)=k_BT\frac{2\pi^4n^2}{(\ln t)^2}. \tag{23}$$

(The corresponding result for absorbing boundary conditions is larger by a factor 2.)

In the presence of quenched randomness, there exists no obvious relation between the free energy and the entropy, and we therefore determined the difference between energies of minimal paths of different winding numbers. The simulation results are depicted in Fig. 9, suggesting a $1/\ln t$ dependence on length, although we cannot rule out some larger power of $1/\ln t$. The slopes of the curves in this figure have ratios of approximately 1/3, 1/6, and 1/2, different from 1/4, 1/9, and 4/9 for an n^2 dependence. We could not collapse the data using the scaling variable $n/\sqrt{\ln t}$ as in Fig. 7. Somewhat surprisingly, the difference in energy vanishes in the large t limit, as in Eq. (23). Naive arguments may have suggested that the energy cost associated with changing the winding number either saturates at a finite value, or possibly even grows as $t^{2\nu-1}$ as in typical energy fluctuations [20]. This

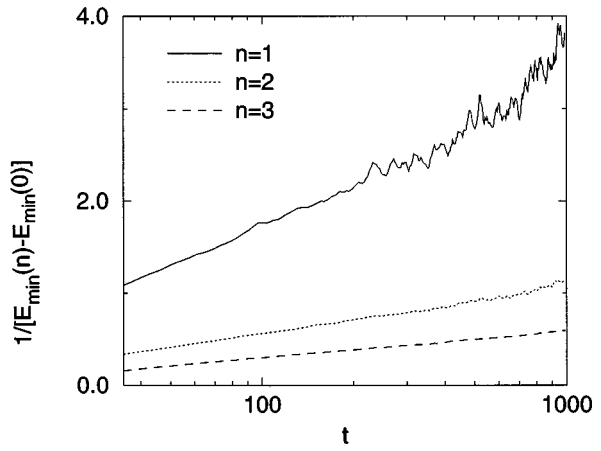

FIG. 9. Difference in minimal energy between directed polymers of different winding numbers as function of the number of time steps t, averaged over 1019 realizations of randomness.

puzzle can be solved by realizing that for large t the FL winds back and forth many times (of the order of $\sqrt{\ln t}$), even when it has a small net winding number of 0 or 1. The fraction of walks of winding number 0 that never make at least half a winding vanishes in the limit $t\to\infty$. However, a walk that has already made half a winding is equally likely to make a further half winding in either positive or negative direction, and therefore the probabilities that the path of minimal energy has winding number 0 or 1 are equal.

Similar results are expected to hold for the windings and entanglements of two FLs around each other. The interactions between the FLs are small at large separations (very small density), and the relative distance between the lines behaves in the same way as the separation of one line from a columnar defect. In the pure system, we had to distinguish between repulsive, neutral, and attractive defects. Since in the presence of point impurities the line does not return to the origin as often, the interaction with the defect is less relevant. In fact, it can be shown that the attraction of the columnar defect must exceed a finite threshold before it can pin a FL [27]. Thus the results of this section regarding the Gaussian distribution of the FL winding angle in the presence of point impurities are expected to hold even for the more realistic attractive columnar pins. Perhaps not surprisingly, the main conclusion is that the pinning to point randomness decreases entanglement.

VI. DISCUSSION AND CONCLUSIONS

Topological entanglements present strong challenges to our understanding of the dynamics of polymers and flux lines. In this paper, we examined the windings of a single FL around a columnar defect. By focusing on even this simple physical situation we were able to uncover a variety of interesting properties: The probability distributions for the winding angles can be classified into a number of universality classes characterized by the presence or absence of underlying symmetries or relevant length scales.

The most ''symmetric'' situation is the windings of an ideal (Brownian) walk around a point center, described by the Cauchy distribution in Eq. (1). Introduction of a finite core for the winding center (or a finite persistence length for the walk) leads to a number of exponentially decaying distributions: If there is a conservation law for the walkers (reflecting boundaries or neutral defects), we obtain the distribution in Eq. (3). Removing this conservation (absorbing boundaries or repulsive defects) leads to the distribution in Eq. (2) whose tails decay twice as fast. Constraining the end points of the walker to the vicinity of the winding center leads to the related distributions in Sec. II D.

A completely new set of distributions is obtained for chiral defects, where the walker is preferentially twisted in one direction at the winding center. These distributions have asymmetric exponential tails, with decay constants that depend on the degree of chirality. Strong chirality appears to lead to quite broad distributions. A remaining challenge is to find the complete form of this probability distribution by solving the two-dimensional diffusion equation with moving boundary conditions.

For nonideal walks, with a vanishing probability to return to the origin, the properties of the winding center are expected to be irrelevant. Both self-avoiding walks in $d=2$ dimensions, and FLs pinned by point impurities in $d=3$, have wandering exponents ν larger than 1/2 and fall in this category. We present a scaling argument (supported by numerical data) that in this the probability distribution has a Gaussian form in the variable $\theta/\sqrt{\ln t}$. Not surprisingly, wandering away from the center reduces entanglement. The characteristic width of the Gaussian form is presumably a universal constant that has been calculated exactly for self-avoiding walks in $d=2$. It would be interesting to see if this constant (only estimated numerically for the impurity pinned FLs in $d=3$) can be related to other universal properties of the walk. Changing the correlations of impurities (and hence the exponent ν) may provide a way of exploring such dependence.

It is likely that there are other universality classes not explored in this paper. The physical problem of FLs in superconductors provides several candidates, such as splayed columnar pins or a collection of pins with random strengths. One example is defects with randomly changing chirality, which induce a change $\pm\Delta\theta$ in winding angle each time the line returns to the defect. Such randomness is in fact irrelevant in the limit $t\to\infty$, since it does not lead to a systematic change of the variable x. The induced variance in x also vanishes as

$$(\delta\Delta x)^2 \simeq \lim_{t\to\infty} \ln t \left(\frac{2\,\delta\Delta\theta}{\ln t}\right)^2 = 0. \tag{24}$$

The underlying problem is certainly quite rich and seems to call for developing some form of renormalization group analysis.

It is also interesting to search for circumstances in which the degree of winding changes dramatically. To compete with the exponential tail of the winding angle distribution, we need an energy proportional to the winding angle itself; a nonlocal quantity. A possible physical realization is provided by a magnetized directed polymer winding around a wire. A current I in the wire generates a magnetic field

$$\vec{B}(\vec{r}) = \frac{2\vec{I}\times\vec{r}}{cr^2},$$

where c is the speed of light. Assuming that the polymer carries a uniform magnetic moment density μ aligned with its backbone, then leads to an energy

$$E = -\mu \int_0^t d\vec{r}(t') \cdot \vec{B}(\vec{r})$$

$$= -\frac{4\pi\mu I n}{c} \equiv \epsilon n,$$

proportional to the winding number n.

In the presence of an energy ϵ per winding, and assuming absorbing boundary conditions, the partition function is given by

$$Z = \int_{-\infty}^{\infty} dn \, \exp\left(-\frac{\epsilon n}{k_B T}\right) \frac{\pi}{4 \cosh^2(2\pi^2 n/\ln t)},$$

where $n = \theta/2\pi$ is the winding number, k_B the Boltzmann constant, and T is the temperature. The integral ''diverges'' if $t \geq t^* = \exp(4\pi^2 k_B T/\epsilon)$, a cutoff only being given by the maximum possible winding number, proportional to t. A directed path, although free on length scales $t < t^*$, is always coiled in the limit of $t \to \infty$. However, for a given length t, a small decrease in temperature can induce a sharp crossover from a free to a coiled configuration due to the exponential dependence of the crossover length t^* on temperature. A similarly sharp crossover occurs for the pinning of a FL to an attractive columnar defect [4] (see Sec. II D). Both transitions are related to the number of returns of a random walk to the origin which scales as $\ln(t)$. We expect similar sharp crossovers between unentangled and braided configurations in other cases, such as several FLs winding around each other.

ACKNOWLEDGMENTS

We thank M.E. Fisher, A. Grosberg, Y. Kantor, P. LeDoussal, and S. Redner for helpful discussions. B.D. was supported by the Deutsche Forschungsgemeinschaft (DFG) under Contract No. Dr 300/1-1. M.K. acknowledges support from NSF Grant No. DMR-93-03667.

[1] P. G. de Gennes, J. Chem. Phys. **55**, 572 (1971).
[2] D. R. Nelson, Phys. Rev. Lett. **60**, 1973 (1988).
[3] M. Rubinstein and S. P. Obukhov, Phys. Rev. Lett. **65**, 1279 (1990).
[4] D. R. Nelson, in *Phase Transitions and Relaxation in Systems with Competing Energy Scales*, edited by T. Riste and D. C. Sherrington (Kluwer Academic, Dordrecht, 1993).
[5] F. Spitzer, Trans. Am. Math. Soc. **87**, 187 (1958).
[6] J. W. Pitman and M. Yor, Ann. Probab. **14**, 733 (1986).
[7] J. F. Le Gall and M. Yor, Probab. Th. Rel. Fields **74**, 617 (1987).
[8] A. Comtet, J. Desbois, and C. Monthus, J. Stat. Phys. **73**, 433 (1993).
[9] K. Itô and H. P. McKean, *Diffusion Processes and Their Sample Paths* (Springer-Verlag, Berlin, 1965).
[10] S. F. Edwards, Proc. Phys. Soc. London **91**, 513 (1967).
[11] F. W. Wiegel, in *Phase Transitions and Critical Phenomena*, edited by C. Domb and J. L. Lebowitz (Academic, London, 1983), Vol. 7.
[12] R. Durett, *Brownian Motion and Martingales in Analysis* (Wadsworth, Belmont, CA, 1984).
[13] M.E. Fisher, V. Privman, and S. Redner, J. Phys. A **17**, L569 (1984).
[14] B. Duplantier and H. Saleur, Phys. Rev. Lett. **60**, 2343 (1988).
[15] J. Rudnick and Y. Hu, Phys. Rev. Lett. **60**, 712 (1988).
[16] J. Rudnick and Y. Hu, J. Phys. A **20**, 4421 (1987).
[17] C. Bélisle, Ann. Probab. **17**, 1377 (1989).
[18] H. Saleur, Phys. Rev. E **50**, 1123 (1994).
[19] A. Grosberg and S. Nechaev, *Polymer Topology*, Advances in Polymer Science Vol. 106 (Springer-Verlag, Berlin, 1993), pp. 1–29.
[20] M. Kardar, Lectures on Directed Paths in Random Media, Les Houches Summer School on Fluctuating Geometries in Statistical Mechanics and Field Theory, August 1994 (Elsevier, North Holland, Amsterdam, in press).
[21] F. B. Knight, *Essentials of Brownian Motion and Diffusion* (American Mathematical Society, Providence, RI, 1981).
[22] A. Comtet, J. Desbois, and C. Monthus, J. Phys. A **26**, 5637 (1993).
[23] G. Blatter, M. V. Feigel'man, V. B. Geshkenbein, A. I. Larkin, and V. M. Vinokur, Rev. Mod. Phys. **66**, 1125 (1994).
[24] B. Houchmandzadeh, J. Lajzerowicz, and M. Vallade, J. Phys. I (France) **2**, 1881 (1992).
[25] J. G. Amar and F. Family, Phys. Rev. A **41**, 3399 (1990).
[26] J. M. Kim, A. J. Bray, and M. A. Moore, Phys. Rev. A **44**, 2345 (1991).
[27] L. Balents and M. Kardar, Phys. Rev. E **49**, 13 030 (1994).